Nanotechnology and Precision Engineering

Investigation into precision engineering design and development of the next-generation brake discs using Al/SiC metal matrix composites

Cite as: Nanotechnol. Precis. Eng. 4, 043003 (2021); https://doi.org/10.1063/10.0007289
Submitted: 29 April 2021 • Accepted: 01 November 2021 • Published Online: 23 November 2021

Jake Haley and Kai Cheng

Nanotechnology and Precision Engineering ARTICLE scitation.org/journal/npe

Investigation into precision engineering design and development of the next-generation brake discs using Al/SiC metal matrix composites

Cite as: Nano. Prec. Eng. 4, 043003 (2021); doi: 10.1063/10.0007289
Submitted: 29 April 2021 • Accepted: 1 November 2021 •
Published Online: 23 November 2021

Jake Haley and Kai Cheng[a]

AFFILIATIONS

Department of Mechanical and Aerospace Engineering, College of Engineering, Design and Physical Sciences, Brunel University London, Uxbridge UB8 3PH, United Kingdom

[a]Author to whom correspondence should be addressed: kai.cheng@brunel.ac.uk

ABSTRACT

Substantially lightweight brake discs with high wear resistance are highly desirable in the automotive industry. This paper presents an investigation of the precision-engineering design and development of automotive brake discs using nonhomogeneous Al/SiC metal-matrix-composite materials. The design and development are based on modeling and analysis following stringent precision-engineering principles, i.e., brake-disc systems that operate repeatably and stably over time as enabled by precision-engineering design. The design and development are further supported by tribological experimental testing and finite-element simulations. The results show the industrial feasibility of the innovative design approach and the application merits of using advanced metal-matrix-composite materials for next-generation automotive and electric vehicles.

KEYWORDS

Brake disc design, Metal matrix composite, Precision engineering design, Tribological testing, Automotive braking system, Finite element analysis (FEA) and simulation

NOMENCLATURE

μ_{pad} pad friction coefficient
A_s disc surface area
H Vickers hardness
H_B Brinell hardness
I sliding distance
K dimensionless wear coefficient
L load
m vehicle mass
p surface pressure
q heat flux
R_{eff} effective radius
$R_{rolling}$ rolling radius
t_s time to stop
V volume removed
v_1 initial velocity
v_{rel} relative velocity
$\dot{\omega}$ rate of volume loss

I. INTRODUCTION

With the era of electric vehicles (either fully electric or hybrid) on the horizon, advanced materials that were not an option in the past because of the demands of traditional braking systems could become more prominent. With regenerative braking being implemented on modern hybrid and fully electric vehicles, energy that would have previously been dissipated as heat through the braking system can now be recovered.

An advantage of Al/SiC metal matrix composite (MMC) over cast iron is that the former is 40% less dense than the latter. Using Al/SiC metal matrix for braking discs has both economic and performance advantages, but the machinability of MMC materials should be better harnessed in their industrial-scale applications.[1,2] If the overall mass of the vehicle is reduced, so is the fuel economy. Figure 1 shows research results obtained by the School of Natural Resources and Environment at the University of Michigan that support this assertion.

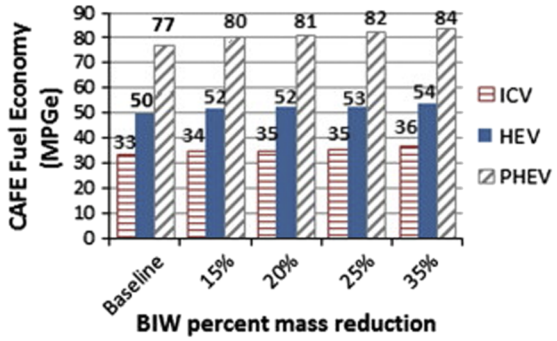

FIG. 1. Fuel-economy results for baseline and lightweight internal combustion vehicles (ICVs), hybrid electric vehicles (HEVs), and plug-in hybrid electric vehicles (PHEVs) (calculated with a gasoline density of 745 kg/m^3).[3]

From a performance perspective, changing to a lighter brake disc reduces the unsprung mass of the vehicle, and keeping the latter to a minimum is desirable because it reduces the forces generated when the vehicle goes over a bump, thereby increasing the ride comfort.[4] A lighter brake-disc system would also improve wheel control by helping the tires maintain contact with the surface. Furthermore, it is essential to use advanced simulations as a virtual design aid for modeling and analyzing automotive brake-disc systems, even at the virtual product stage.[5,6]

Additionally, the tribological properties of the materials must be considered in the context of a precision-engineering product. The interactions between the brake disc and brake pad are a key aspect of a braking system and exhibit intrinsic multiphysics phenomena in the interfacial actions. These interactions are also a common cause of many brake-system failures, such as brake fade. Being able to compare the tribological properties of the brake-disc materials would enable designers to make better-informed decisions about the best materials for particular applications. Therefore, developing advanced simulations on a virtual brake-disc system and a corresponding well-designed experimental study are expected for designing and developing next-generation brake-disc systems promptly and robustly.[7–9]

Based on this information, if the conclusion is that Al/SiC MMC is a suitable alternative material, then there is scope to improve both vehicle performance and fuel economy. Therefore, we undertook the present research and development in collaboration with a Formula One industrial company to develop next-generation brake discs that would be particularly applicable to electric vehicles. In this paper, the following core work is presented in detail, supported by in-depth analysis, simulations, and experimental studies.

(1) Design and analysis of a brake disc made from Al/SiC MMC such that it has comparable or better performance than that of a cast-iron brake disc for a given application. To be successful, the Al/SiC MMC disc must be (i) at least 50% lighter, (ii) reach acceptable temperatures in all braking scenarios, and (iii) undergo acceptable displacements in all braking scenarios.
(2) Developing a precision-engineering design approach by combining precision-engineering principles with finite element analysis (FEA) modeling and simulations, which enables accurate analysis and comparison of the wear-resistance characteristics of complex nonhomogeneous MMC materials.
(3) Undertaking systematic tribological testing and assessment against industrial requirements, particularly for the future generation of automotive and electric vehicles.

II. PRECISION-ENGINEERING DESIGN AND ANALYSIS OF BRAKE DISCS

The brake discs were designed and analyzed following precision-engineering principles, i.e., ensuring that the designed brake discs can operate repeatably and stably over time. The thermal and mechanical analyses featured in the investigation presented herein were conducted using FEA models and simulations. The design method was focused on using advanced precision-engineering analysis that bridges the gaps among the physical brake-disc/braking system, physical modeling, analytical/mathematical models, and computational results. Consequently, the design and analysis are linked tangibly and closely to the physical disc system and its optimal design.

A. Methodology

Initially, brake discs that are currently in production were analyzed for the intended application. The same brake-disc design was then used but with Al/SiC MMC used as the material to enable direct comparison between the two types of discs and materials. This would also identify any areas for design development. The two materials compared are 150-grade cast iron[10] and F3S.20S, which has a percentage composition of 20% SiC particles and an average particle size of 12.8 μm.[11] The material properties are summarized in Table I.

Figure 2 shows a CAD image of the brake disc, along with its key geometrical dimensions. This disc is used in a two-seater sports car from the industrial collaborator, and the key vehicle parameters needed for the analysis are given in Table II.

With this information, the boundary conditions for the thermal and mechanical analyses can be derived. For the thermal analysis, the heat flux must be determined, which can be calculated as

$$q(\mathrm{W/m^2}) = \frac{m(\mathrm{kg}) \times v_1^2\left(\frac{\mathrm{m}}{\mathrm{s}}\right) \times \text{Dynamic axle mass}_{\text{front/rear}}(\mathrm{kg})}{4 \times \text{Total dynamic mass}\ (\mathrm{kg}) \times t_s(\mathrm{s}) \times A_s(\mathrm{m^2})}. \quad (1)$$

To calculate the mechanical boundary conditions, the clamping force applied on the disc to achieve a certain deceleration must be determined. This is done by first calculating the amount of braking torque needed, followed by the clamping force:[12]

$$\text{Clamp force}_{\text{front/rear}}(\mathrm{N}) = \frac{m(\mathrm{kg}) \times \text{Ideal braking ratio}_{\text{front}} \times (z \times 9.81) \times R_{\text{rolling}}(\mathrm{mm})}{\left(4 \times R_{\text{eff}}(\mathrm{mm}) \times \mu_{\text{pad}}\right)}. \quad (2)$$

TABLE I. Material properties used for analysis.

Property	Symbol	Unit	Material	
			Cast iron (150 grade)	Duralcan F3S.20S
Density	ρ	kg/m^3	7000	2765
Young's modulus	E	GPa	100	99
Tensile strength	T_s	MPa	150	359
Yield strength	Y_s	MPa	98	338
Specific heat capacity	c	J/(kg K)	595	1084
Thermal conductivity	λ	W/(m K)	60	201
Max. operating temperature	MOT	°C	1000	450
Hardness	H	Pa	5.55×10^8	4.80×10^8
Emissivity	ε		0.81	0.37

To understand the thermal capabilities of the materials in-depth, several scenarios must be simulated. Herein, an aggressive singular-stop event and a multiple-stop event are simulated. A singular stop causes the disc to absorb a large amount of energy over a short time; this gives a final temperature known as the singular-stop temperature rise (SSTR), which is a key characteristic of a brake disc. The multiple-stop simulation allows inspection of the disc's ability to disperse heat, through both its material choice and design. For the mechanical study, a static structural simulation was run, in which a clamping force was applied to the disc to inspect its displacement. The parameters for the singular braking event are given in Table III.

To simulate multiple braking events, the vehicle firstly brakes from a speed of 26.82 m/s (60 mph) to rest at a deceleration of 1g, then 0.1 s later, it accelerates back up to speed before braking again; this is repeated for a total of five braking events. For more-realistic brake application, we wait for 0.1 s before applying the heat flux. An overview of the boundary conditions for the thermal and mechanical analyses is shown in Fig. 3.

An unknown in the thermal study was the heat transfer coefficient (HTC). This was determined through CFD simulation, and an average value was taken on each of the brake faces and imported into the ANSYS Mechanical model. The modeling technique used to determine the HTC was similar to that used by Belhocine and Omar.[13]

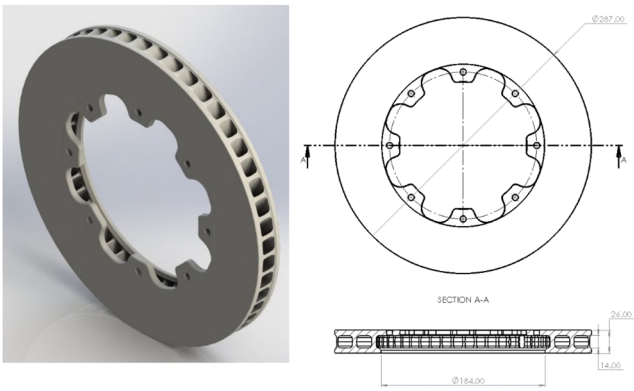

FIG. 2. Baseline brake-disc design being analyzed.

B. Validation of thermal model

To validate the thermal model, the SSTR for 150-grade cast iron was calculated analytically as

$$\mathrm{SSTR}_{\mathrm{front}} = T_\infty(\mathrm{K}) + \left(\frac{\text{Energy per wheel}_{\mathrm{front}}(\mathrm{J})}{\text{Specific Heat Capacity}(\mathrm{J/kg\ K}) \times m_T(\mathrm{kg})}\right). \tag{3}$$

TABLE II. Key vehicle parameters.

Design parameter	Value		Units
Vehicle data			
Wheelbase	2 301		mm
Vehicle weight	11 909		N
Vehicle mass	1 214		kg
CoG height	450		mm
Weight distribution	Front	Rear	⋯
	0.38	0.62	
Front axle mass	461.37		kg
Rear axle mass	752.70		kg
Max. speed	68.84		m/s
Rolling radius	Front	Rear	mm
	297	312.6	
0–60 time	4.3		s
Disc data			
Disc OD	288		mm
Disc ID	184		mm
Disc effective radius	119		mm
Pad friction coefficient	0.4		⋯
Thermal mass	4.07		kg
Disc thickness	26		mm
Airgap	14		mm

TABLE III. Singular-stop parameters.

Parameter		Value	Units
Deceleration	z	$1g$	m/s^2
Initial velocity	v_1	68.84	m/s
Final velocity	v_2	0	m/s
Ambient temperature	T_∞	298.15	K

Comparison between the analytical calculation and the thermal simulation showed a percentage difference of ~2% for the front disc and ~3% for the rear disc.

C. Analytical results and further analysis

The results in Table IV support the research conducted previously by Grieve *et al.*,[14] who showed that cast iron performed better for a short aggressive stop. A visual inspection of the screenshots in the Appendix shows clearly that the temperature distribution with Al/SiC MMC is better than that with cast iron. If the temperature difference between the center of the brake face and the edge is examined, F3S.20S gives a temperature difference of ~80 °C, which is better than the temperature difference of 140 °C

TABLE IV. Comparison of singular-stop temperature rise (SSTR).

	SSTR, analytical [°C]		SSTR, simulation [°C]	
Material	Front	Rear	Front	Rear
Cast iron (150 grade)	367	277	360	265
Duralcan F3S.20S	496	373	470	357

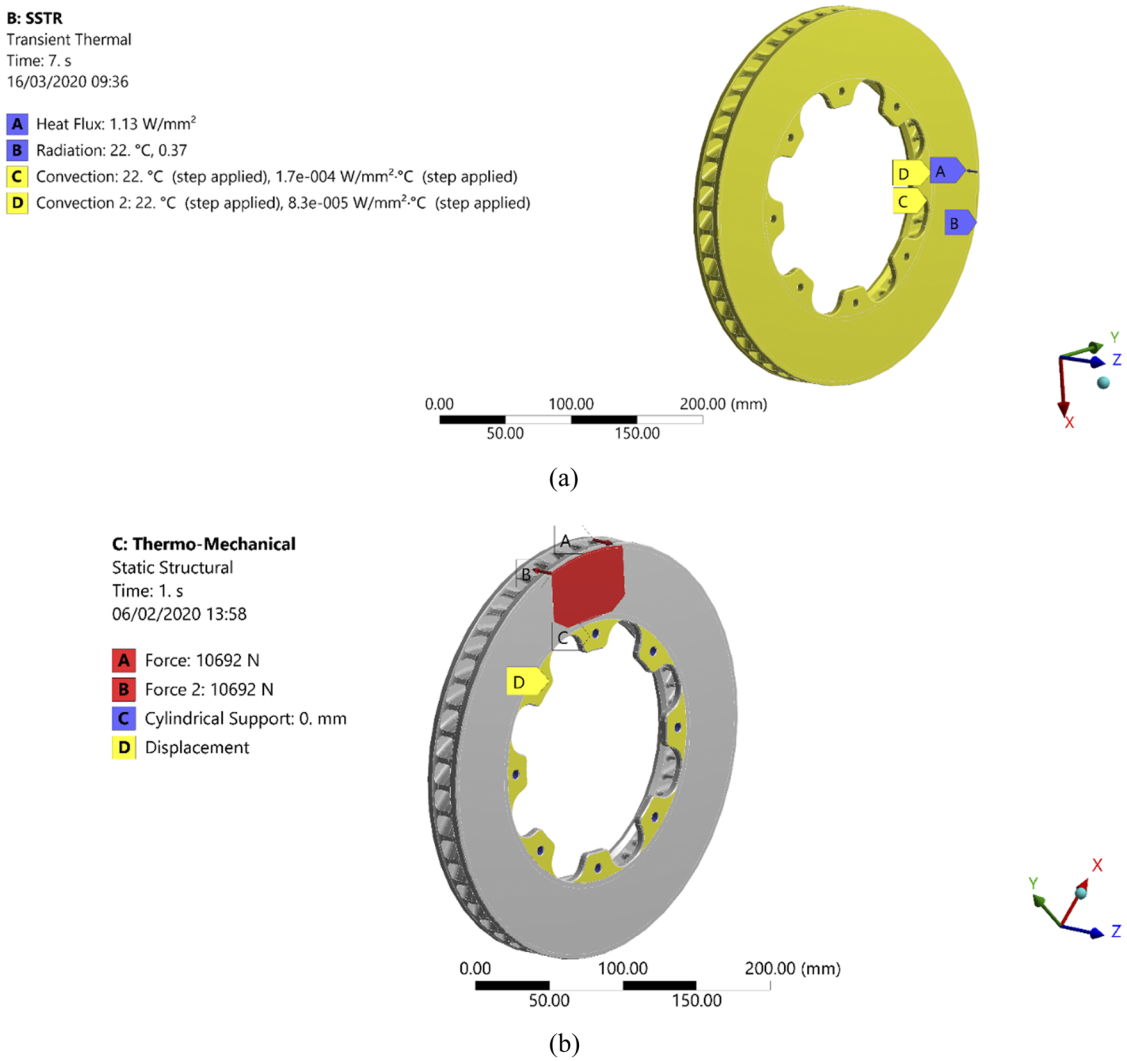

FIG. 3. Boundary conditions for (a) thermal and (b) mechanical analyses.

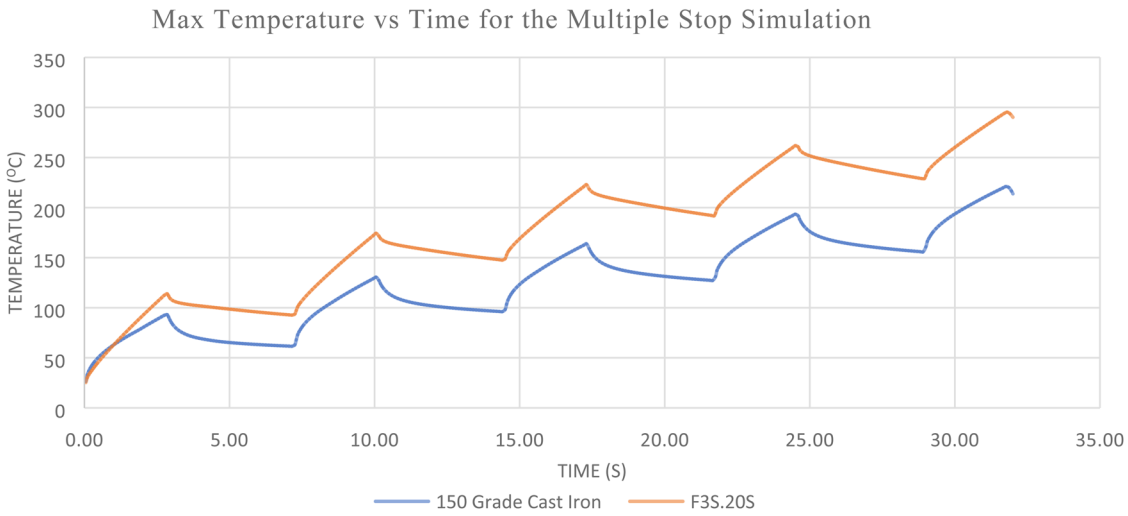

FIG. 4. Results for temperature with multiple stops (front disc application).

seen with cast iron. This improved distribution would help to prevent the formation of "hot spots," leading to more-consistent braking performance. If the temperature difference between the disc face and the lugs is also inspected, the temperature gradient with cast iron (~333 °C) is greater than that with F3S.20S (~265 °C). This smaller temperature gradient would help to prevent thermal cracking, as outlined by Mackin *et al.*[15] Therefore, the present results build on the conclusions reached in previous research, given that the temperature gradient has been decreased successfully. This and the fact that F3S.20S has a yield strength of roughly three and a half times greater suggest that thermal cracking would be less common if F3S.20S was to be used as the brake-disc material. Visual and analytical inspection of the heat distribution on brake discs is absent in many research reports. Being able to reduce the chance of hot spots forming would increase the consistency of braking performance, this is because excessive disc-face temperature can influence the coefficient of friction between the disc and the pad. Eliminating thermal cracking would also reduce the chance of brake failure, prolonging the life of the product and making it both safer and more sustainable.

If F3S.20S is to be used on the front axle, then it is evident that further design development of the current disc design is needed to enable a more comparable final temperature. Upon inspection of the SSTR equation [Eq. (3)], the only way to decrease the SSTR would be to increase the thermal mass. Given that F3S.20S is more than 50% lighter (see Table I), this means that there is space for material to be added, which could potentially make the brake disc suitable for a front application.

Figure 4 shows that over the five 60–0-mph stops, cast iron performed best because it had the lowest final temperature at the end of the stops. This was expected because cast iron had the best SSTR performance and the cooling of the brake disc is independent of material. What is interesting to note is that after each stop, the delta area between the temperatures increased when comparing F3S.20S to cast iron. This was unexpected because the hypothesis was that the higher thermal conductivity of Al/SiC MMC would

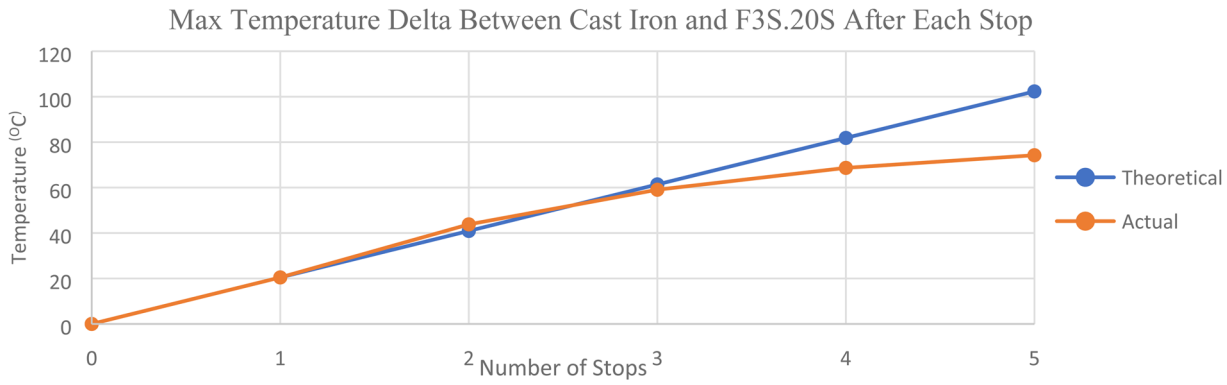

FIG. 5. Comparison between predicted and actual delta between cast iron and F3S.20S (front disc application).

TABLE V. Mechanical simulation results.

Material	Max. displacement [mm]
150-grade cast iron	0.004 04
F3S.20S	0.004 03

help to distribute heat over the brake disc, thereby decreasing the maximum temperature by the temperature being more uniform. Then again, if the delta after the first stop is used to predict the temperature after the next four stops, it is evident that the delta does in fact decrease. Figure 5 shows evidence of this, suggesting that the higher thermal conductivity of Al/SiC MMC is helping to distribute the temperature as the number of braking events increases. This also suggests that thermal conductivity has a greater influence at higher temperatures because, over the first three stops, there is no noticeable difference between the theoretical and actual delta.

These results show that if Al/SiC MMC is to have comparable performance to that of cast iron for multiple stops, the disc design requires some development. The cooling properties of the disc must be improved to enable it to reach a lower temperature in between the braking events, and increasing its thermal mass would provide a smaller temperature change between stops. The thermal performance of the MMC-based disc is also coupled with its tribological and mechanical performances, which should be addressed appropriately in the context of multiphysics-based modeling and analysis.

Table V shows that cast iron has a higher maximum displacement than that of 40% Al/SiC MMC. A lower maximum displacement allows for a more uniform pressure distribution across the brake pad during operation, potentially leading to more-consistent braking performance. A low maximum displacement was also a key characteristic of a brake disc as outlined by Awe.[16] This suggests that switching to Al/SiC MMC would improve the mechanical performance of the brake disc, with the smaller displacement helping to prevent failure modes such as disc judder.

III. DEVELOPMENT OF BRAKE DISCS

Based on the thermal analysis and further analysis taking account of the thermomechanical coupling effects, design changes were made to improve the performance of the baseline disc when F3S.20S was used as the material. The changes included increasing the disc thickness and decreasing the air gap to increase the thermal mass of the disc. The same studies were run again to compare the improvements and determine whether the developed design is suitable for the application.

A. Results

Figure 6 shows the maximum temperatures reached with cast iron and F3S.20S used for the baseline disc and F3S.20S used for the developed disc. Clearly, the developed disc outperforms the baseline F3S.20S disc. Also, the developed disc reaches a temperature that is 23 °C higher for the front and 29 °C higher for the rear when compared to the baseline cast-iron disc. The design modifications have also enabled F3S.20S to be used on the front axle, as the temperature reached is 67 °C below the MOT (Ministry of Transport) test requirement.

Figure 7 shows the temperature distribution of the developed disc at the end of the SSTR braking event. When compared with the Appendix, there is evidently a slight decrease in the temperature gradient between the center of the brake-disc face and the outer edge. The developed disc has a temperature gradient of ~60 °C, whereas the baseline disc has a temperature gradient of 80 °C with F3S.20S and 140 °C with cast iron. This slight improvement will further aid in preventing hot spots from forming on the brake-disc surface.

If the temperature gradient between the center of the disc face and the lugs is investigated, then the developed disc also sees an improvement over the baseline disc. It is observed that the

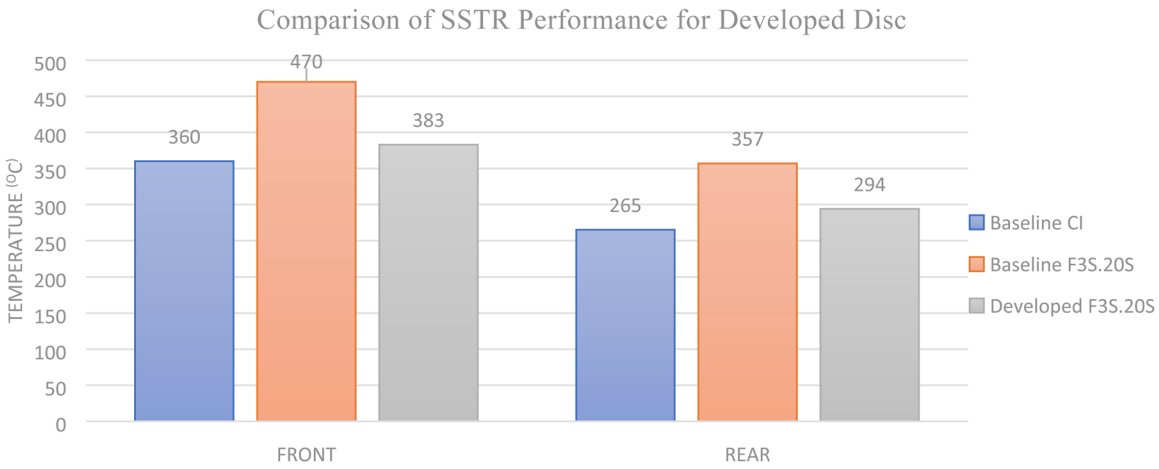

FIG. 6. Comparison of maximum temperature reached during single-stop braking event.

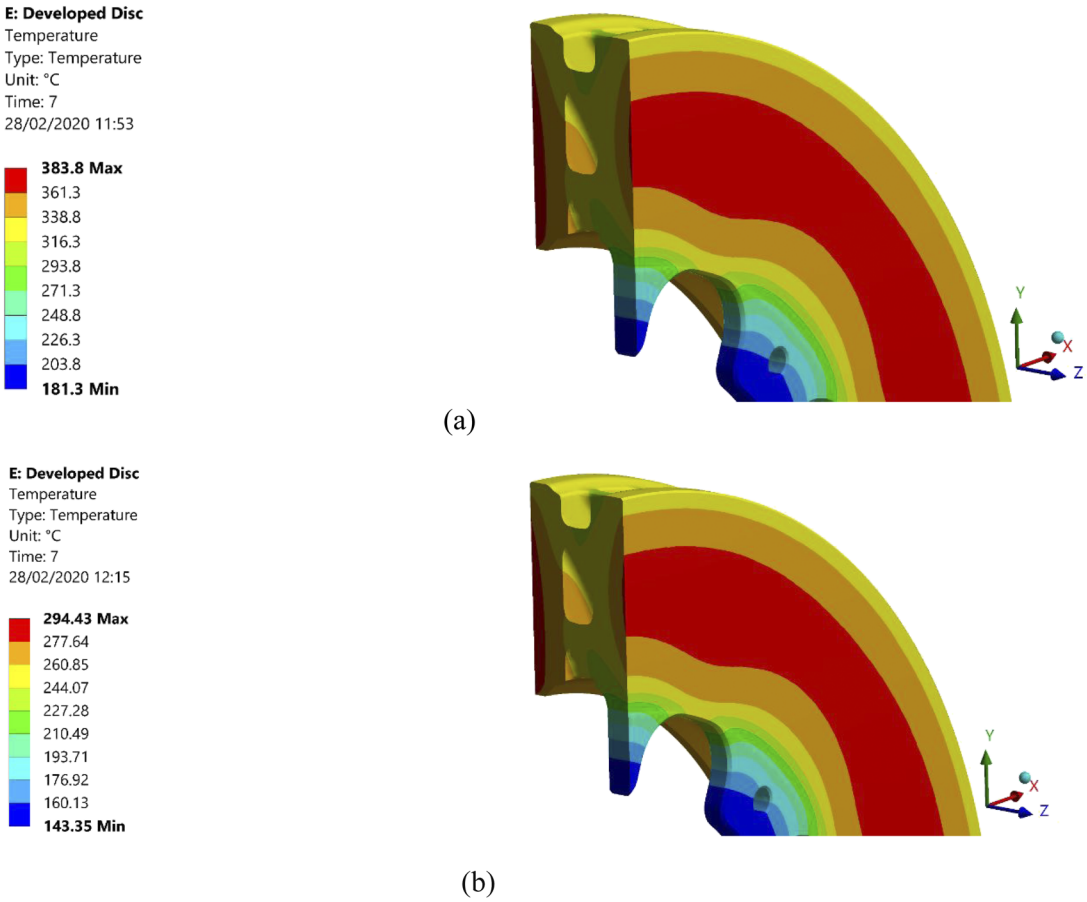

FIG. 7. Simulation results showing single-stop performance of developed disc: (a) front application; (b) rear application.

developed disc has a temperature gradient of ~200 °C, whereas the baseline disc has a temperature gradient of 265 °C (F3S.20S) and 333 °C (cast iron). This suggests that the extra material added to the brake-disc face has aided the temperature distribution, which helps to prevent thermal cracking and improves the tribological performance of the disc because the temperature distribution is coupled with the tribological and mechanical properties at the interfacial surfaces. The complex interfacial interactions can be modeled and further analyzed by using multiphysics-based virtual simulations.

B. Multiple-stop performance

Figure 8 compares how the maximum temperature changes across multiple braking events. The graph shows that the developed disc outperforms the F3S.20S baseline disc but not the cast-iron baseline disc. Over the first two stops, the maximum temperatures at the end of the braking events for the 150-grade cast iron and the developed disc are similar. However, the better single-stop performance of the cast-iron baseline means that the delta between the maximum temperatures of the two discs increases slowly. The final delta for the developed disc is 30 °C, which is still comparable given the small percentage difference between the values (~12%).

Figure 9 shows the deltas for both the baseline (F3S.20S) and developed disc; clearly, they both increase after each braking event. With more braking events, the delta begins to plateau in both cases, meaning that the delta between the cast-iron baseline and the developed disc will not be excessive after more braking events. This supports the findings shown in Fig. 5, where the reason for the delta plateauing is the higher thermal conductivity acting at higher temperatures. The developed disc has a lower delta in all scenarios, which is expected based on the trend seen in Fig. 8.

C. Mechanical performance

Despite the acceptable mechanical performance of the baseline Al/SiC MMC disc, the mechanical study of the developed disc was run using the boundary conditions outlined in Fig. 3. This was done to see if any improvements were made. Table VI gives the results.

The results show that the developed disc has improved mechanical performance, which is expected considering that material has

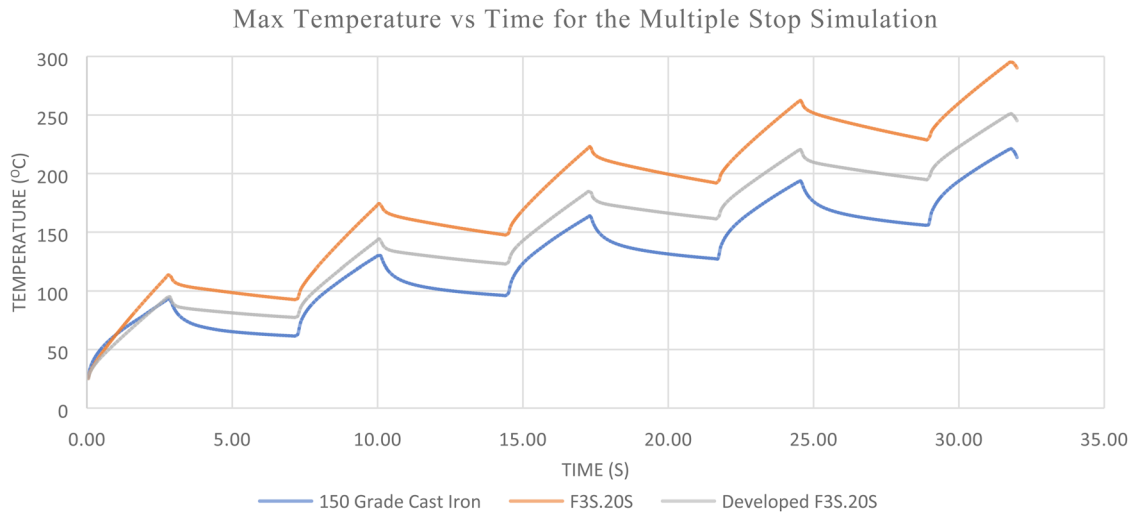

FIG. 8. Comparison of maximum temperature after each braking event in multiple-stop simulation.

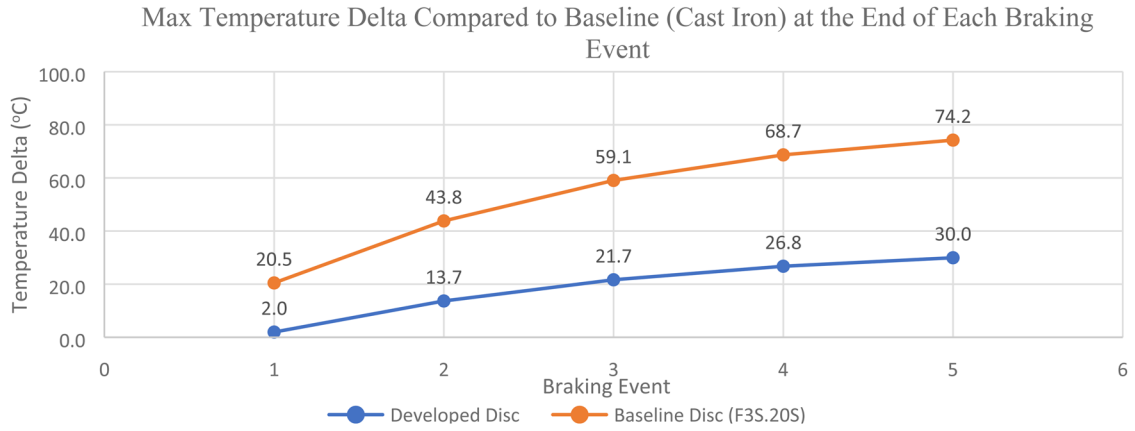

FIG. 9. Delta of baseline: cast-iron disc compared to baseline, F3S.20S, and developed disc at end of each braking event.

been added, which would warrant an increase in stiffness. The developed disc also has a lower maximum stress than that of the best-performing baseline material, but it still has a higher maximum displacement. However, the developed disc is 30% stiffer and has an 8.3% lower maximum stress when compared to the cast-iron baseline disc, thus proving that the developed disc has better mechanical performance.

TABLE VI. Comparison of mechanical performance.

Disc	Max. displacement [mm]	Max. stress [MPa]
Baseline (cast iron)	0.004 04	27.50
Baseline (F3S.20S)	0.004 03	27.30
Baseline (40% Al MMC)	0.002 68	27.17
Developed (F3S.20S)	0.002 99	25.30

IV. TRIBOLOGICAL DEVELOPMENT AND ASSESSMENT

Before simulating the wear of a brake disc, an accurate model must first be developed. An experiment known as the "pin-on-disc" experiment was conducted and replicated in ANSYS Mechanical, where the theory applied to the "pin-on-disc" model was then transferred to a brake pad and disc model to compare the wear characteristics of the two materials.

A. Physical testing

Photographs of the Al/SiC MMC samples used for the physical testing and the tribometer that was used are shown in Fig. 10.

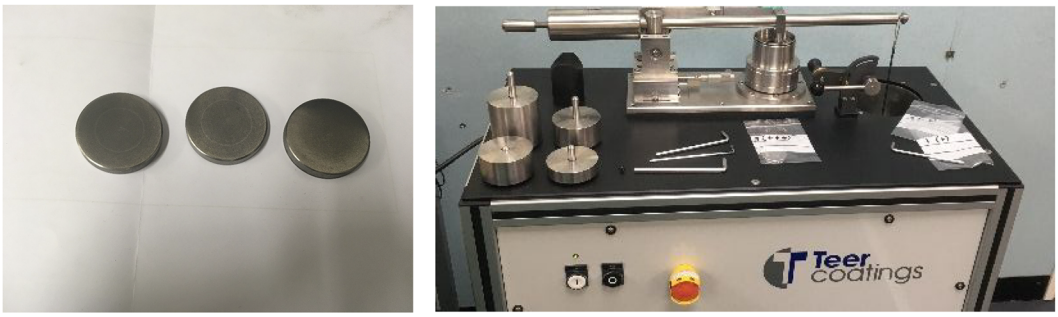

FIG. 10. Sample discs (left) and tribometer used for physical testing (right).

The tribometer measured the friction force and coefficient of a sample by rotating it while applying a vertical load to the top face of the disc via a pin. During this operation, the frictional contact between the pin and the disc pushed the pin against the probe by which the tribometer measured the friction force. This friction force was then plotted against time, thereby enabling correlation between the physical testing and the simulation.

This experiment also allowed calculation of the dimensionless wear coefficient K:[17]

$$K = \frac{3 \times H_B \times V(\mathrm{m}^3)}{I(\mathrm{m}) \times L(\mathrm{N})}. \tag{4}$$

The only unknown in Eq. (4) is the removed volume V, which can be calculated by inspecting the trough left behind by the pin, as shown schematically in Fig. 11. To find the area hatched in green, the angle θ must first be determined, which by trigonometry is given as

$$\theta = 2 \times \left(\sin^{-1} \left(\frac{r}{(\text{Trough Width}/2)} \right) \right). \tag{5}$$

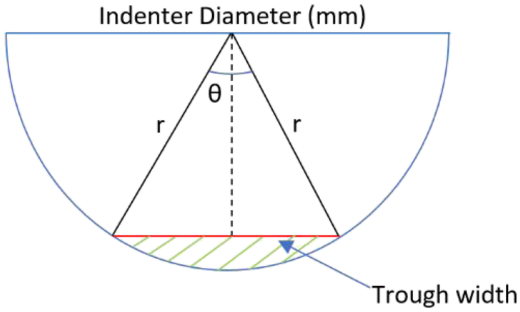

FIG. 11. Schematic of trough left behind by pin.

The trough width was measured using an electronic microscope after the experiment had been conducted; the width was measured at several locations for a more accurate result. With the angle determined, the area can then be calculated as

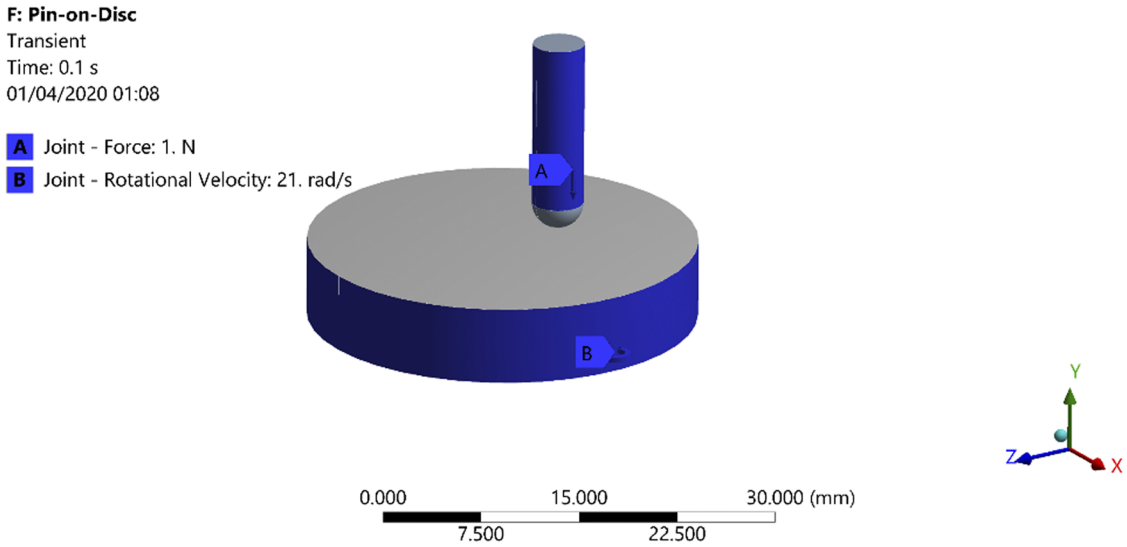

FIG. 12. Illustration of "pin-on-disc" simulation and boundary conditions.

$$\text{Area} = \frac{1}{2} \times r^2 \times (\theta - \sin(\theta)). \quad (6)$$

With the area calculated, the removed volume can be found by multiplying the area by the circumference around the diameter of the track, which was set by the experiment. Figure 12 shows the variables set for the experiment and simulation.

B. FEA simulation

The simulation was developed using ANSYS Mechanical combined with the analysis using other engineering tools. To replicate the pin-on-disc experiment, additional APDL (ANSYS Parametric Design Language) commands were added, applying Archard's wear law to simulate the wear on the disc. The model used for the simulation is shown in Fig. 12.

According to the ANSYS manual,[18] the equation that is applied through the APDL commands is

$$\dot{w} = \frac{K}{H} \times p^n \times v_{\text{rel}}{}^m, \quad (7)$$

where n and m are constants bespoke to the problem. First, within the contact association between the pin and the disc, additional material properties and constants were defined using APDL commands as shown in Fig. 13. The values of n and m used in this problem were derived using the information found in the ANSYS user manual.[18] An overview of the boundary loads is shown in Fig. 14.

To apply rotational velocity to the disc, a body–ground revolute joint was applied to allow its rotation axially with all other degrees of freedom restrained. A body–ground translational joint was also added to the pin to allow vertical translation but restrain all other degrees of freedom. A force of 10 N was then applied to the pin to replicate the force applied on the tribometer.

C. Results

Figure 15 shows a clear correlation between the experimental and simulated "pin-on-disc" results. Note that because of excessive simulation times, the first 5 s of the simulation were used to predict the remaining 295 s through linear interpolation. In reality, the friction force would not increase linearly because of the shape of the pin; however, because of the small wear depth seen in physical testing, it can be assumed to be linear. The reliability of the interpolated results could also be questioned. This is because the interpolation used 1.67% of the overall time to predict the other 98.33%, which means that a small error in the initial 1.67% could have a massive effect overall. Despite this, the final percentage difference of ~15% after 300 s is acceptable given the points mentioned.

```
K=0.000124 !determine experimentally through experiment
H=480  !hardness, MPA
n=1  !exponent on contact pressure
m=1  !exponent on relative pressure velocity

TB,WEAR,cid,,,ARCD !activating Archard's Wear Law
TBFIELD,TIME,0
TBDATA,1,0,H,n,m !wear not occurring from t=0 to t=2
TBFIELD,TIME,2
TBDATA,1,0,H,n,m
TBFIELD,TIME,2.01
TBDATA,1,K,H,n,m !wear occurring from t=2.01s onwards
TBFIELD,TIME,302
TBDATA,1,K,H,n,m !302 to allow for 300s of wear
```

FIG. 13. APDL commands added to contact set.

D. Further tribological analysis

The theory was then applied to a brake disc and pad model, where the boundary conditions were provided for the simulation as illustrated in Fig. 16.

Figure 17 shows the wear taking place on the disc during its first half rotation. The wear progresses from ~2.65×10^{-5} to ~9.59×10^{-5} as the force acting on the pad is ramped up over the first 1-s time step. The wear is then consistent for the first rotation until it encounters an already deformed mesh, where it then deforms further, representing wear taking place. This image also shows how the whole brake face does not wear, which is expected because the pad does not fully cover the whole braking face.

Figure 18 compares the wear depth between Al/SiC MMC and cast iron against time. F3S.20S has a higher wear resistance than does

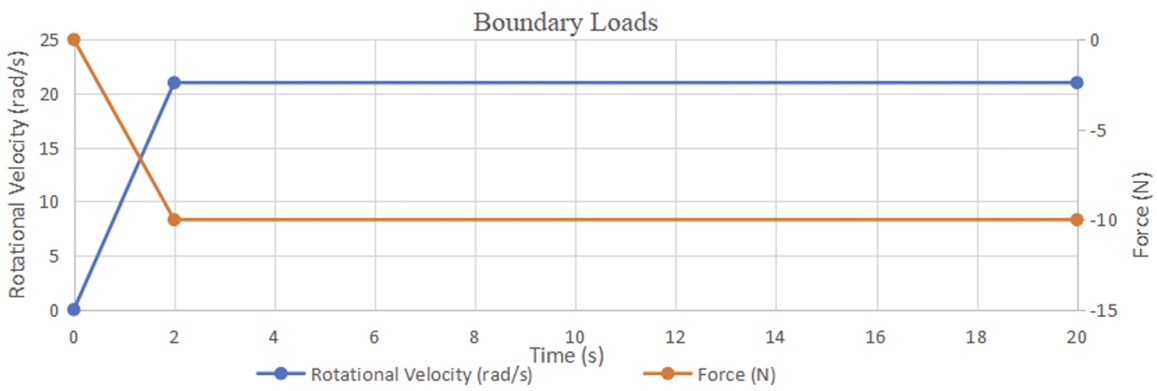

FIG. 14. Boundary loads applied to model over time (graph terminated at 20 s for clarity).

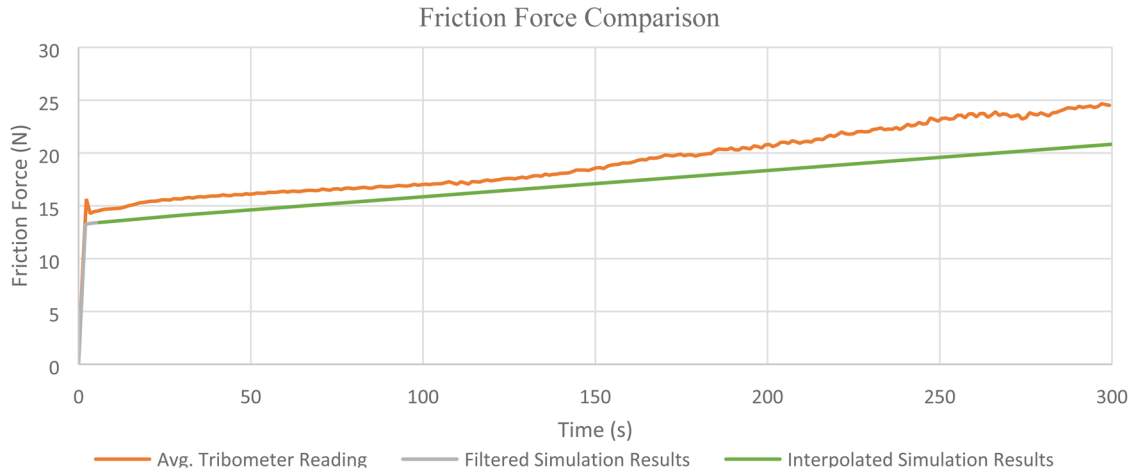

FIG. 15. Comparison between physical and simulated "pin-on-disc" experiment.

cast iron, which is surprising considering that cast iron is harder than F3S.20S. However, the corresponding K value for F3S.20S is lower. Also, the wear relationship for both materials is linear, which is expected because the cross section in contact with the disc is constant. The relationship found in this research correlates with that in previous physical research, which showed that Al/SiC MMC has a better resistance to wear.[19]

In the present research and development, we further developed the modeling and simulations following multiphysics-based analysis principles combined with precision-engineering design and analysis of the MMC disc as a product, while focusing on the interfacial actions at the brake-disc surface. The multiphysics covers thermal, tribological, and material science aspects, which are coupled in the modeling and analysis. However, one aspect that was not investigated in this research is the implementation of temperature into the wear simulation. This is also a limitation that was outlined regarding the Archard wear equation.[20] If this was to be investigated, it could show that the wear resistance of Al/SiC MMC decreases because of the "scoring" that has been noted in previous research.[21] Previous physical testing has been conducted to evaluate the wear resistance of Al/SiC MMC at elevated temperatures.[22] This research and development only conducted tests up to temperatures of 200 °C,[22] although it can be seen from the thermal studies conducted that temperatures easily exceed this. Work is still underway with the simulations and experimental study and is expected to be reported separately in the near future.

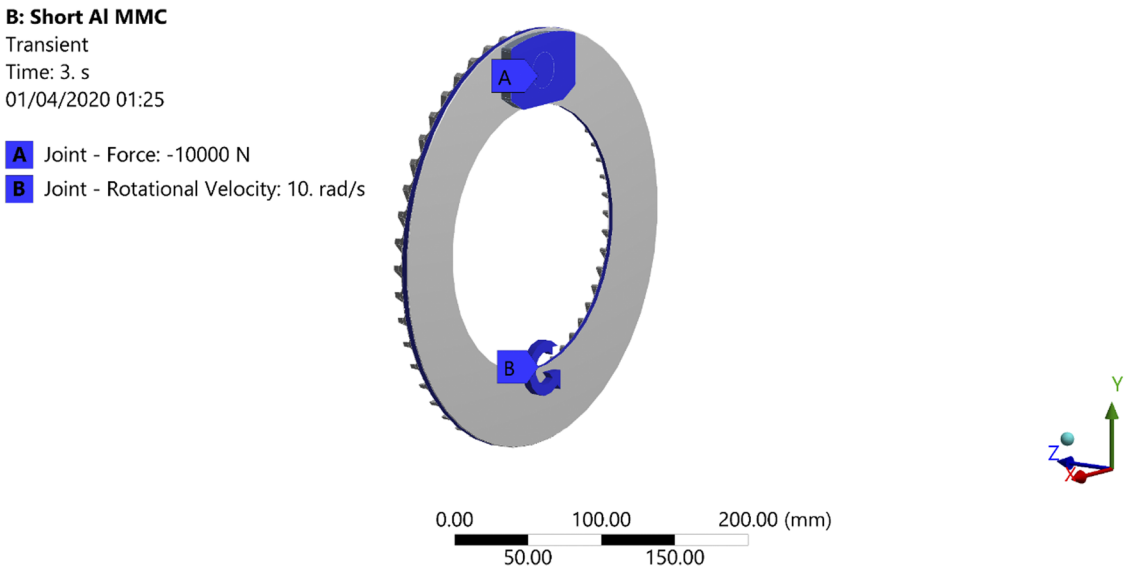

FIG. 16. Illustration of boundary conditions for simulation.

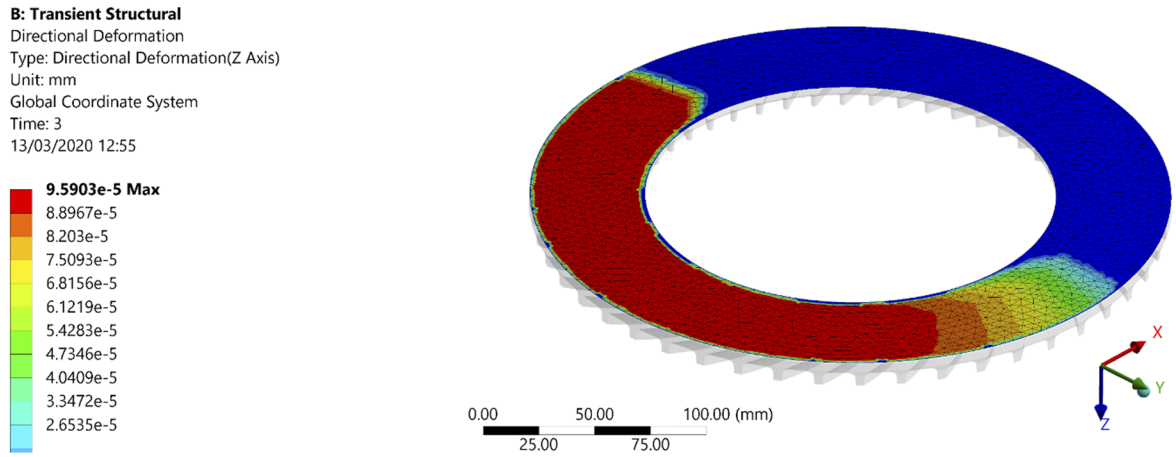

FIG. 17. Illustration of progressive wear occurring on brake disc.

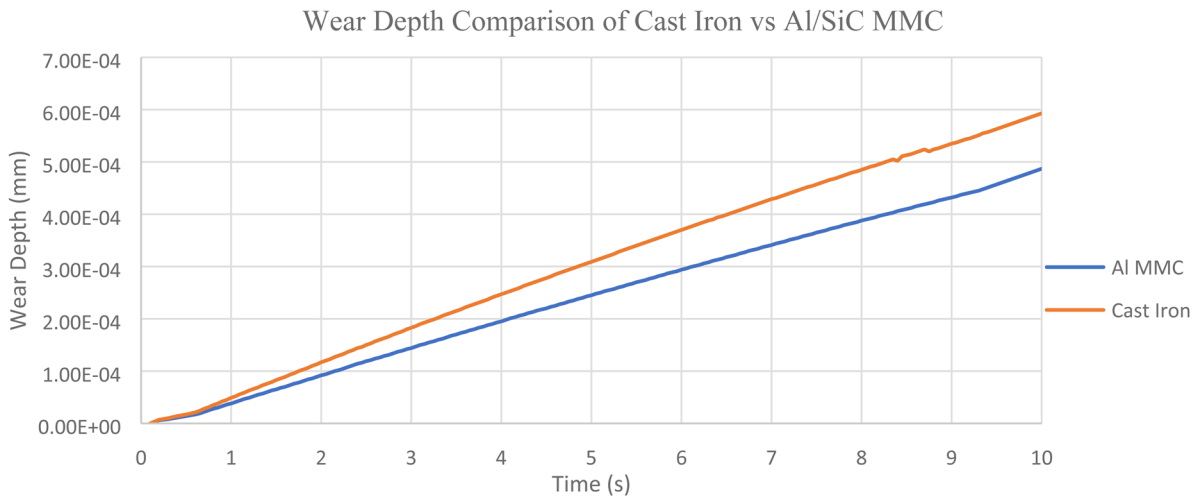

FIG. 18. Wear-depth comparison over time between Al/SiC MMC and cast iron (accelerated wear).

V. CONCLUSIONS

This paper has presented the precision-engineering design and analysis of innovative brake discs made of advanced Al/SiC MMC materials. FEA-based thermal and mechanical studies of the disc design were carried out following multiphysics-based modeling and analysis combined with precision-engineering design principles, aimed at a high degree of accuracy and harnessing the complexity in using nonhomogeneous materials in the product design and development. This research and development enabled the accurate comparison of cast iron and F3S.20S (Al/SiC MMC) for use on an automotive brake-disc system. Tribological testing and assessment were undertaken with suitable correlation to physical "pin-on-disc" testing to further evaluate and validate the disc's design. With suitable thermal performance and better tribological performance on wear resistance, friction effect, and air lubrication and cooling capacity, Al/SiC MMC-based discs are shown to be industrially feasible for next-generation automotive brake-disc systems. A weight saving of 50% can also be achieved in prototyping the brake-disc system with much-improved engineering performance. The approach and development work presented herein have the potential for broad precision-engineering design and analysis of engineering products using advanced nonhomogeneous engineering materials in particular, and for increasingly stringent and complex precision-engineering applications.

ACKNOWLEDGMENTS

The authors are grateful for the experimental support received from research centers (BCAST and ETC) at Brunel University London and for the product-design support received from the industrial partner.

AUTHOR DECLARATIONS

Conflict of Interest

The authors have no conflicts to disclose.

DATA AVAILABILITY

The authors confirm that the data supporting the findings of this study are available within the article.

APPENDIX: IMAGES OF BASELINE DISC AT END OF SINGULAR-STOP BRAKING EVENT

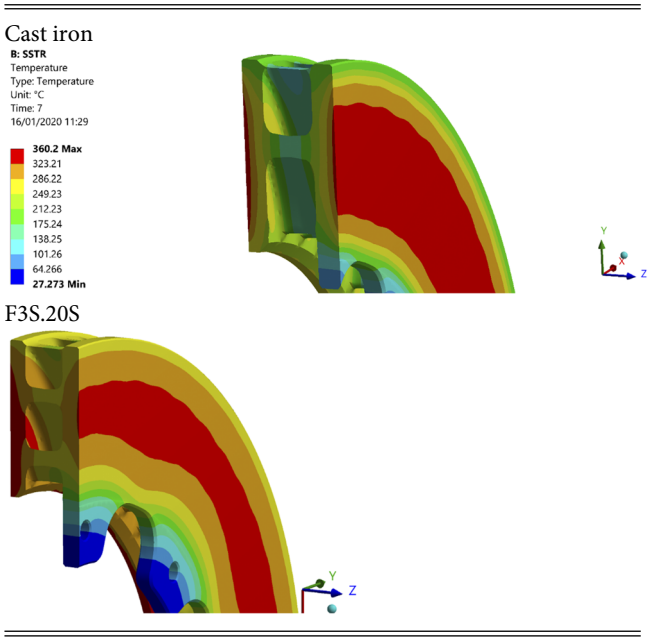

REFERENCES

[1] Niu Z, Cheng K. Improved dynamic cutting force modelling in micro milling of metal matrix composites part II: Experimental validation and prediction. Proc Inst Mech Eng Part C 2020;234(8):1500–1515. https://doi.org/10.1177/0954406219893725.

[2] Cheng K. Machining dynamics: Theory, applications and practices. London: Springer. 2008.

[3] Lewis AM, Kelly JC, Keoleian GA. Vehicle light weighting vs. electrification: Life cycle energy and GHG emissions results for diverse powertrain vehicles. Appl Energy 2014;126:13–20. https://doi.org/10.1016/j.apenergy.2014.03.023.

[4] Livesey A. Practical motorsport engineering. 1st ed. Oxon: Routledge. 2019. Vol. 200–201. p. 220.

[5] Belhocine A, Abdullah OI. Design and thermomechanical finite element analysis of frictional contact mechanism on automotive disc brake assembly. J Failure Anal Prev 2020;20:270–301. https://doi.org/10.1007/s11668-020-00831-y.

[6] Belhocine A, Omar WZW. Three-dimensional finite element modelling and analysis of the mechanical behaviour of dry contact slipping between the disc and the brake pads. Int J Adv Manuf Technol2017;88(1):1035–1051. https://doi.org/10.1007/s00170-016-8822-y.

[7] Belhocine A, Ghazaly NM. Effects of Young's modulus on disc brake squeal using finite element analysis. Int J Acoust Vib 2016;21(3):292–300. https://doi.org/10.20855/ijav.2016.21.3423.

[8] Belhocine A. FE prediction of thermal performance and stresses in an automotive disc brake system. Int J Adv Manuf Technol 2017;89:3563–3578. https://doi.org/10.1007/s00170-016-9357-y.

[9] Shao YZ, Adetoro M, Cheng K. Development of multiscale multiphysics-based modelling and simulations with the application to precision machining of aerofoil structures. Eng Comput 2021;38(3):1330–1349. https://doi.org/10.1108/ec-10-2019-0473.

[10] Fallon M. Data handbook for grey irons. 1st ed. Birmingham: Butterworth-Heinemann. 1997. pp. 17–40.

[11] F3S.20S product specification. 2nd ed. 1993.

[12] Day A Braking of road vehicles. London: Butterworth-Heinemann Ltd. 2014.

[13] Belhocine A, Omar WZW. CFD analysis of the brake disc and the wheel house through air flow: Predictions of surface heat transfer coefficients (SHTC) during braking operation. J Mech Sci Technol 2018;32(1):481–490. https://doi.org/10.1007/s12206-017-1249-z.

[14] Grieve DG, Barton DC, Crolla DA, Buckingham J. Design of a lightweight automotive brake disc using finite element and Taguchi techniques. Proc Inst Mech Eng Part D 1998;212(4):245–254. https://doi.org/10.1243/0954407981525939.

[15] Mackin TJ, Noe SC, Ball KJ, et al. Thermal cracking in disc brakes. Eng Failure Anal 2002;9(1):63–76. https://doi.org/10.1016/s1350-6307(00)00037-6.

[16] Awe SA. Developing material requirements for automotive brake disc. Mod Concepts Mater Sci 2019;2(2);1–4.

[17] Yang LJ. Wear coefficient equation for aluminium-based matrix composites against steel disc. Wear 2003;255(1–6):579–592. https://doi.org/10.1016/s0043-1648(03)00191-1.

[18] ANSYS mechanical user manual. 2019. Chap. 43.3.1.1, available at https://ansyshelp.ansys.com/account/secured?returnurl=/Views/Secured/corp/v194/ans_tec/tecwearmodel.html?q=wear (Accessed 1 March 2020).

[19] Metal matrix composites: Custom-made materials for automotive and aerospace engineering. In: Kainer KU: Wiley. 2006.

[20] ResearchGate. What are the limitations of the Archard wear equation?. 2018, available at https://www.researchgate.net/post/What_are_the_limitations_of_Archard_wear_equation (Accessed 14 February 2020).

[21] Oda N, Sugimoto Y, Higuchi T, Minesita K. Development of disc brake rotor utilizing aluminium metal matrix composite. Warrendale, PA: Society of Automotive Engineers. 1997. Technical Paper 970787.

[22] Abhik R, Umasankar V, Xavior MA. Evaluation of properties for Al-SiC reinforced metal matrix composite for brake pads. Procedia Eng 2014;97:941–950. https://doi.org/10.1016/j.proeng.2014.12.370.

Professor Kai Cheng is a Chair Professor in Manufacturing Systems at Brunel University London. His current research interests focus on design of high-precision machines, ultraprecision and micro/nano manufacturing, multiscale multiphysics-based modeling and analysis, smart tooling, and smart machining. He is also currently leading the Micro/Nano Manufacturing Theme at Brunel University London, which involves 12 academic staff, five postdoctoral fellows, and about 40 Ph.D. students. Professor Cheng and his team have been working closely with industrial companies in the UK, Europe, USA, and the Far East. They are working on a number of research projects funded by the EPSRC, NATEP Program, RAEng, Innovate UK Program, EU Horizon 2020 Programs, and industry. Professor Cheng is a Charted Engineer and a Fellow of the IMechE and IET, and the European editor for the International Journal of Advanced Manufacturing Technology.